JOURNAL OF BACTERIOLOGY, Apr. 2006, p. 2392–2399 Vol. 188, No. 7
0021-9193/06/$08.00+0 doi:10.1128/JB.188.7.2392–2399.2006


# Identification of a Novel α-Galactosidase from the Hyperthermophilic Archaeon *Sulfolobus solfataricus*†

Stan J. J. Brouns,[1]* Nicole Smits,[1] Hao Wu,[1] Ambrosius P. L. Snijders,[2] Phillip C. Wright,[2] Willem M. de Vos,[1] and John van der Oost[1]

*Laboratory of Microbiology, Department of Agrotechnology and Food Sciences, Wageningen University, Hesselink van Suchtelenweg 4, 6703 CT Wageningen, The Netherlands,[1] and Biological and Environmental Systems Group, Department of Chemical and Process Engineering, University of Sheffield, Mappin Street, Sheffield S1 3JD, United Kingdom[2]*

Received 4 November 2005/Accepted 16 January 2006

***Sulfolobus solfataricus*** **is an aerobic crenarchaeon that thrives in acidic volcanic pools. In this study, we have purified and characterized a thermostable α-galactosidase from cell extracts of *S. solfataricus* P2 grown on the trisaccharide raffinose. The enzyme, designated GalS, is highly specific for α-linked galactosides, which are optimally hydrolyzed at pH 5 and 90°C. The protein consists of 74.7-kDa subunits and has been identified as the gene product of open reading frame Sso3127. Its primary sequence is most related to plant enzymes of glycoside hydrolase family 36, which are involved in the synthesis and degradation of raffinose and stachyose. Both the *galS* gene from *S. solfataricus* P2 and an orthologous gene from *Sulfolobus tokodaii* have been cloned and functionally expressed in *Escherichia coli*, and their activity was confirmed. At present, these *Sulfolobus* enzymes not only constitute a distinct type of thermostable α-galactosidases within glycoside hydrolase clan D but also represent the first members from the *Archaea*.**

α-Galactosidases (α-Gals) (EC 3.2.1.22) are a widespread class of enzymes that liberate galactose from the nonreducing end of sugars. In bacteria, yeasts, and fungi, these enzymes are usually involved in the degradation of various plant saccharides, which can then serve as a carbon and energy source for growth. Plants synthesize α-galactosides such as raffinose and stachyose as the major energy storage molecules in leaves, roots, and tubers. Moreover, these oligosaccharides have been associated with cold and desiccation tolerance of seeds (28). Both raffinose and stachyose are produced by two specialized synthases (raffinose synthase [EC 2.4.1.82] and stachyose synthase [EC 2.4.1.67]) that use galactinol as a galactosyl donor (39). The oligosaccharides are degraded during seed germination by the action of two distinct types of α-Gals that differ in their optimal pH of catalysis. While the acid α-Gal type is most likely active in the acidic environment of the vacuole and the apoplasm, the alkaline α-Gal type probably catalyzes galactose release in the more neutral or alkaline cytoplasm (4, 17, 31). Mammals express an α-Gal and an α-*N*-acetylgalactosaminidase (α-NAGal) in lysosomal bodies to degrade glycolipids, glycoproteins, and oligosaccharides. In humans, mutations in the X-chromosomal α-Gal gene can lead to an accumulation of these α-linked galactosides in tissues, which results in a recessive disorder called Fabry disease (12). Mutations in the related α-NAGal gene, which is located on chromosome 22, lead to either Schindler or Kanzaki disease.

Glycoside hydrolases (GHs) have been classified into families based on their primary sequence similarities (23). Except for some rare cases (34), the majority of α-Gals can be found in GH clan D (GH-D), which comprises families 27 and 36. The two families share a fairly conserved catalytic domain and hydrolyze the glycosidic bond with retention of configuration of the liberated D-galactose (3). Substantial insight into the molecular mechanisms of substrate recognition and catalysis of these enzymes was acquired when the crystal structures of the human, rice, and fungal α-Gals (16, 18, 20), as well as the chicken α-NAGal (19), were obtained.

In this study, we have purified an unusual intracellular α-Gal from the hyperthermophilic crenarchaeon *Sulfolobus solfataricus* P2, an aerobic microorganism that lives in terrestrial volcanic pools of high acidity (75 to 85°C, pH 2 to 4) (2).

## MATERIALS AND METHODS

All chemicals were of analytical grade and purchased from Sigma, unless stated otherwise. Primers were obtained from MWG Biotech AG (Ebersberg, Germany). PCRs were performed with *Pfu* TURBO polymerase (Stratagene). The chromogenic substrate X-α-Gal (5-bromo-4-chloro-3-indolyl-α-D-galactopyranoside) was purchased from Glycosynth (Warrington, United Kingdom).

**Growth of *Sulfolobus* species.** *S. solfataricus* P2 (DSM1617) and *S. tokodaii* (JCM10545) were grown aerobically at pH 3.5 in a rotary shaker at 80°C. The medium contained 2.5 g/liter $(NH_4)_2SO_4$, 3.1 g/liter $KH_2PO_4$, 203.3 mg/liter $MgCl_2 \cdot 6\ H_2O$, 70.8 mg/liter $Ca(NO_3)_2 \cdot 4\ H_2O$, 2 mg/liter $FeSO_4 \cdot 7\ H_2O$, 1.8 mg/liter $MnCl_2 \cdot 4\ H_2O$, 4.5 mg/liter $Na_2B_4O_7 \cdot 2\ H_2O$, 0.22 mg/liter $ZnSO_4 \cdot 7\ H_2O$, 0.06 mg/liter $CuCl_2 \cdot 2\ H_2O$, 0.03 mg/liter $Na_2MoO_4 \cdot 2\ H_2O$, 0.03 mg/liter $VOSO_4 \cdot 2\ H_2O$, and 0.01 mg/liter $CoCl_2 \cdot 6\ H_2O$ and was supplemented with 3 g/liter carbon source and Wollin vitamins.

The Wollin vitamin stock (100×) contained 2 mg/liter D-biotin, 2 mg/liter folic acid, 10 mg/liter pyridoxine-HCl, 10 mg/liter riboflavin, 5 mg/liter thiamine-HCl, 5 mg/liter nicotinic acid, 5 mg/liter DL-Ca-pantothenate, 0.1 mg/liter vitamin $B_{12}$, 5 mg/liter *p*-aminobenzoic acid, 5 mg/liter lipoic acid.

**Purification of the α-Gal from *S. solfataricus* P2 extracts.** A 3.6-liter culture of *S. solfataricus* P2 was grown on raffinose to an $A_{600}$ of 0.8, after which the cells were centrifuged (10 min, 6,000 × *g*, 4°C). The cell pellet (8.8 g [wet weight]) was resuspended in 10 ml of 50 mM Tris-HCl (pH 7.5) and frozen at −80°C. After thawing, the cells were sonicated and diluted 1:1 in the same buffer containing 1 mM phenylmethylsulfonyl fluoride. The suspension was clarified by centrifugation (60 min, 19,000 × *g*, 4°C). All subsequent chromatographic steps were

* Corresponding author. Mailing address: Laboratory of Microbiology, Department of Agrotechnology and Food Sciences, Wageningen University, Hesselink van Suchtelenweg 4, 6703 CT Wageningen, The Netherlands. Phone: 31-317-483110. Fax: 31-317-483829. E-mail: stan.brouns@wur.nl.

† Supplemental material for this article may be found at http://jb.asm.org/.

TABLE 1. Strains, plasmids, and primers used in this study

| Strain, plasmid, or primer | Entry code/genotype, description, or sequence (5′→3′)[a] | Reference, source, or restriction site/codon change |
|---|---|---|
| *S. solfataricus* P2 | DSM1617 (wild type) | 46 |
| *S. tokodaii* strain 7 | JCM 10545 (wild type) | 44 |
| *E. coli* HB101 | $F^-$ *hsdS*20 ($r_B^-$ $m_B^-$) *ara-14 galK2 lacY1 leuB6 mcrB mtl-1 proA2 recA13 rpsL20 supE44 thi-1 xyl-5* ($Str^r$) | 1 |
| *E. coli* BL21(DE3)-RIL | *hsdS gal*(λ*c*I*ts*857 *ind1Sam7 nin5 lacUV5*-T7 gene *1*) | Novagen |
| Plasmids | | |
| pET24d | T7 RNA polymerase expression system | Novagen |
| pMAL-CT | N-terminal fusion tag of *E. coli* MBP | New England Biolabs |
| pWUR269 | *galS* (Sso3127) in pET24d (BspHI/NcoI-XhoI) | This study |
| pWUR270 | *galSt* (St2554) in pET24d (NcoI-BamHI) | This study |
| pWUR271 | *galS* (Sso3127) in pMAL-CT (BamHI-PstI) | This study |
| pWUR272 | pWUR271 with substitution D367G | This study |
| pWUR273 | pWUR271 with substitution D425G | This study |
| Primers | | |
| *galS*-fw (Sso3127) | CGTGATCATGATTTGGATAGAAGACGAGAATGGG | BspHI |
| *galS*-rv (Sso3127) | GCTCACTCGAGTCATTCTATAGTAACTGGGATTCC | XhoI |
| *galSt*-fw (St2554) | GGGCGCCATGGCTATTTGGATATATGATGAAAATGGG | NcoI |
| *galSt*-rv (St2554) | GCCCGGGATCCTTACTCGATACTAACTATTTCTTCAGC | BamHI |
| MBP-*galS*-fw (Sso3127) | CGCGGATCCATGATTTGGATAGAAGACGAG | BamHI |
| MBP-*galS*-rv (Sso3127) | CCGCGCTGCAGTCATTCTATAGTAACTGGGATTCC | PstI |
| *galS*-fw D367G[b] | **G**TAATCAATGGGTAATTCACGC | GAT→GGT |
| *galS*-rv D367G[b] | CAACCTTAACGAGATCGAAG | GAT→GGT |
| *galS*-fw D425G[c] | GAGGAATTCTATAG**G**CTACGTACCCTTC | GAC→GGC |
| *galS*-rv D425G[c] | GAAGGGTACGTAG**C**CTATAGAATTCCTC | GAC→GGC |

[a] Restriction sites are underlined, and nucleotide mismatches are indicated in boldface.
[b] Excite mutagenesis primer (Stratagene).
[c] QuikChange mutagenesis primer (Stratagene).

performed on an ÄKTA fast protein liquid chromatography system (Amersham Biosciences) at room temperature.

First, the supernatant was applied to a 70-ml Q-Sepharose Fast Flow (Amersham Biosciences) anion exchange column which was equilibrated with 50 mM Tris-HCl (pH 7.5). After extensive washing, the proteins were eluted by a linear gradient of buffer with 0.5 M NaCl. Active fractions were pooled and dialyzed overnight against 10 mM $NaP_i$ buffer (pH 6.8). The dialyzed fraction was then loaded onto a hydroxyapatite column, CTH5-I (Bio-Rad), and eluted by a linear gradient of 500 mM $NaP_i$ buffer (pH 6.8). Fractions that contained α-Gal activity were pooled, dialyzed overnight against 50 mM $NaP_i$ buffer (pH 6.8), and applied to a MonoQ 5/50 GL column (Amersham Biosciences). The proteins were eluted by a linear gradient of 50 mM $NaP_i$ buffer (pH 6.8) supplemented with 0.5 M NaCl. Subsequently, the pooled MonoQ fractions were purified by gel filtration chromatography using a Superdex 200 HR 10/30 column (Amersham Biosciences) and 50 mM $NaP_i$ buffer (pH 6.8) supplemented with 100 mM NaCl.

**Protein identification.** The protocol to identify the α-Gal was slightly modified from that of Snijders et al. (42, 43). Coomassie-stained protein bands were excised with a scalpel from a sodium dodecyl sulfate (SDS)-polyacrylamide gel and transferred to low-adhesion Eppendorf tubes. Next, they were destained twice with 200 mM $NH_4HCO_3$ in 40% acetonitrile (ACN) for 30 min at 37°C. After this, the gel pieces were shrunk with ACN and dried in a vacuum centrifuge, and the proteins were reduced with 10 mM dithiothreitol (DTT) (30 min, 56°C) and alkylated with 50 μl of 55 mM iodoacetamide in 50 mM $NH_4HCO_3$ (20 min at room temperature in the dark). After this, gel pieces were washed with 50 mM $NH_4HCO_3$ and shrunk with ACN. Next, the trypsin solution was added, consisting of 8 μg of trypsin in 100 μl of 9% ACN and 50 mM $NH_4HCO_3$ (overnight at 37°C). The next day, peptides were extracted in four sequential extraction steps: (i) 50 μl of 50 mM $NH_4HCO_3$ (10 min at room temperature), (ii) 75 μl of ACN (15 min at 37°C), (iii) 75 μl of 5% formic acid (FA), and (iv) 75 μl of ACN (15 min at 37°C). Extracts were pooled and dried down to completeness in a vacuum centrifuge, and peptides were redissolved in 0.1% formic acid and 3% ACN. The peptide mixture was separated on a PepMap $C_{18}$ RP capillary column (LC Packings, Amsterdam, The Netherlands) and eluted directly onto a QStarXL electrospray ionization–quadrupole time-of-flight (ESI qQ-TOF) tandem mass spectrometer (Applied Biosystems/MDS Sciex). Gradients and data acquisition were set up as previously described (42, 43). A database search was performed with Mascot 2.0 (www.matrixscience.com) against the Mass Spectrometry Protein Sequence DataBase. The peptide tolerance was set to 1.0 Da, and the tandem mass spectrometry tolerance was 0.6 Da. Carbamidomethyl modification of cysteine was set as a fixed modification, and methionine oxidation was set as a variable modification. A maximum of one missed cleavage site by trypsin was allowed.

**Protein quantitation.** Protein concentrations were determined by using the bicinchoninic acid protein assay (Pierce) and the Bradford assay (Bio-Rad) according to the supplied protocol.

**Enzyme assays.** Standard activity assays were performed with 1.0 mM pNPG (*para*-nitrophenol-α-D-galactopyranoside) in a 50 mM citric acid–$Na_2HPO_4$ buffer (pH 5.0) at 80°C. The reaction was stopped by adding 0.7 volumes of cold 1 M $Na_2CO_3$, after which the sample was put on ice. The amount of released *para*-nitrophenol (pNP) was measured at 420 nm and calculated with an extinction coefficient of 0.0135 $\mu M^{-1}\ cm^{-1}$ (33). One unit of activity was defined as the amount of enzyme required to convert 1 μmol of pNP per minute. Thermal inactivation assays were performed by incubating 45 μg/ml of enzyme at 70, 80, and 90°C and drawing aliquots at regular intervals during 2.5 h. The residual activity was then determined by the standard assay. The optimal pH of the enzyme was determined with the McIlvaine citrate-phosphate buffer system (36) in a pH range of 2.2 to 8.0. Several pNP-substituted hexoses and pentoses were tested as a substrate at a concentration of 20 mM under standard conditions.

The activity toward the disaccharide melibiose [D-galactose-α(1,6)-D-glucose], the trisaccharide raffinose [D-galactose-α(1,6)-D-glucose-(α1,β2)-D-fructose], and the tetrasaccharide stachyose [D-galactose-α(1,6)-raffinose] (Fluka) was tested in a continuous assay at 80°C using 20 mM of substrate and 0.4 mM $NADP^+$ in a 50 mM $NaP_i$ buffer (pH 7.0). The amount of liberated D-galactose was measured by adding 20 U of *Thermoplasma acidophilum* glucose dehydrogenase (Sigma) and calculated with an extinction coefficient of 6.22 $mM^{-1}\ cm^{-1}$ for NADPH (33).

The effects of different divalent metal ions, EDTA, and DTT were tested at a concentration of 10 mM in a standard assay. Sugars such as D-galactose, sucrose, L-arabinose, and D-fucose were analyzed for inhibitory effects at concentrations of 5, 10, and 25 mM.

**Gene cloning and mutagenesis.** The genomic fragments corresponding to Sso3127 and St2554 were PCR amplified from genomic DNA that was prepared

TABLE 2. Purification of the native *S. solfataricus* α-Gal

| Step | Protein (mg) | Activity (U) | Sp act (U mg$^{-1}$) | Purification factor | Recovery (%) |
|---|---|---|---|---|---|
| Cell extract | 174 | 31.5 | 0.18 | 1 | 100 |
| Q-Sepharose | 49 | 19.5 | 0.4 | 2 | 62 |
| Hydroxyapatite | 7 | 7.8 | 1.16 | 6 | 25 |
| MonoQ | 3 | 6.4 | 2.31 | 13 | 20 |
| Superdex | 0.26 | 1.1 | 4.25 | 23 | 4 |

according to the method of Pitcher et al. (40), and the amplified genes were cloned into vector pET24d or pMAL-CT, respectively, using *Escherichia coli* HB101 as a host (Table 1). Mutations were introduced by employing either the Excite or QuikChange protocols (Stratagene). Inserts of plasmids used in this study were sequenced by Westburg Genomics (Leusden, The Netherlands).

**Recombinant protein overexpression and purification.** Plasmids pWUR269 and pWUR270, containing the *galS* gene from *S. solfataricus* P2 and the *galSt* gene from *S. tokodaii*, respectively, were transformed into *E. coli* BL21(DE3)-RIL. Transformants were grown overnight at 37°C and used to inoculate 1-liter cultures that were incubated to an $A_{600}$ of approximately 0.8. The cultures were then placed on ice to induce cold shock proteins which may prevent inclusion body formation (7). After 1 h, recombinant protein expression was induced by adding 0.5 mM IPTG (isopropyl-β-D-thiogalactopyranoside). The cultures were allowed to grow for 4 h at room temperature, after which the cells were centrifuged.

Plasmids pWUR271, pWUR272, and pWUR273, containing wild-type and mutant α-Gal genes translationally fused to the *E. coli* maltose binding protein (MBP), were transformed into *E. coli* HB101, and the protein was overexpressed as described above. Frozen cell pellets were resuspended in 20 mM Tris-HCl (pH 7.5) buffer which was supplemented with 150 mM NaCl, 10% (vol/vol) glycerol, and complete protease inhibitors (Roche). Cell suspensions were then sonified (Branson sonifier) while the sample was kept in an ice-ethanol bath at −10°C. Next, insoluble cell matter was removed by centrifugation (60 min, 26,500 × *g*, 4°C). Clarified cell extracts were then loaded onto equilibrated amylose resin (New England Biolabs). After extensive washing with the same buffer without glycerol and protease inhibitors, the fusion protein was eluted in buffer supplemented with 10 mM maltose. To concentrate the fusion protein and to remove contaminating maltose, the sample was diluted five times in NaCl-free buffer and loaded onto a MonoQ 5/50 GL column (Amersham Bioscience). Pure fusion proteins were eluted by a linear gradient of the same buffer with 1 M NaCl. MBP was removed by thrombin cleavage according to the instructions from the manufacturer (Sigma), after which the recombinant GalS was reisolated by MonoQ as described above.

**Sequence analysis of α-Gals.** A total of 171 α-Gal sequences belonging to PF0265 and PF05691 were obtained from the Pfam database. A small subset of sequences, including the ones for which a crystal structure is available and selected members of the different subgroups of GH-D, was then aligned using the TCoffee program (38). Additional sequences were subsequently added to the alignment using the ClustalX profile alignment mode. Extensive manual alignment editing was performed with the BioEdit software package, after which highly similar sequences were discarded. Neighbor-joining trees of 43 representative sequences were then calculated and bootstrapped in ClustalX, while correcting for multiple substitutions. Trees were drawn with the program Treeview. Sequence motifs comprising the catalytic nucleophile and acid/base were made using the Weblogo server (8).

## RESULTS

**Purification and identification of the α-Gal from *S. solfataricus*.** *S. solfataricus* P2 is capable of using α-linked galactosides such as melibiose and raffinose as a sole carbon and energy source. The capability to do so requires the presence not only of a suitable sugar uptake system but also of an intracellular α-Gal and an efficient metabolic pathway for stepwise oxidation of the released monosaccharides. Activity assays using extracts of *S. solfataricus* grown on several sugars, as well as tryptone, confirmed the presence of a constitutively expressed enzyme which is capable of hydrolyzing pNPG. The α-Gal was purified from 8.8 g of cells, which were harvested from a 3.6-liter late-exponential-phase culture grown on raffinose. In four subsequent chromatographic steps (Q-Sepharose, hydroxyapatite, MonoQ, and Superdex), the specific activity was enriched 23-fold (Table 2). The enriched fractions were found to contain two major protein bands, of approximately 73 and 87 kDa, by SDS-polyacrylamide gel electrophoresis (PAGE) (Fig. 1, top). Size exclusion chromatography showed that the α-Gal eluted in fractions corresponding to proteins of a native molecular mass of 225 ± 15 kDa, suggesting a trimeric oligomerization (data not shown). Separations of the α-Gal using columns based on hydrophobic interactions resulted in an almost complete loss of activity. Similarly, affinity purification using immobilized D-galactose (Pierce) proved unsuccessful, since the enzyme did not bind to the resin. Therefore, the protein could not be purified to apparent homogeneity. To identify their corresponding genes, both major protein bands were excised and treated with trypsin, after which the peptides were eluted from the gel slice, desalted, concentrated, and analyzed by ESI qQ-TOF tandem mass spectrometry. Twenty-one different peptides (40% sequence coverage, MOWSE score of 831) were found that matched band 1 with the gene product of Sso2760 (*cutA-5*), an 84.9-kDa protein which is orthologous to the 80.5-kDa α-subunit of the aldehyde oxidoreductase of *S. acidocaldarius* (26). In band 2, 17 unique peptides were found that matched the gene product of Sso3127 (Uniprot, Q97U94), a 74.6-kDa hypothetical protein that shares sequence similarity with raffinose synthases and seed

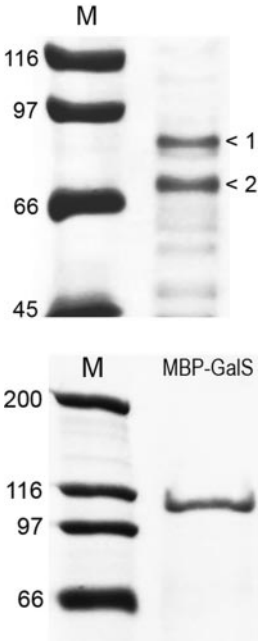


FIG. 1. (Top) Purification of the native α-Gal from *S. solfataricus*. A digital photograph of an 8% SDS-PAGE gel loaded with 5 μg total protein of the α-Gal enriched fraction after gel filtration chromatography is shown. The gel was stained with Coomassie brilliant blue G250. The sizes of the broad-range protein marker are shown in kilodaltons. Arrows 1 and 2 indicate the two protein bands that were identified by mass spectrometry. (Bottom) Digital photograph of a 6% SDS-PAGE gel loaded with 2 μg GalS fusion protein after affinity and anion exchange chromatography.

imbibition proteins of GH36. The MOWSE score for this protein was 517, and a sequence coverage of 34% was achieved. This protein was deemed likely to be responsible for the thermostable α-Gal activity and was termed GalS.

**Characteristics of native GalS. (i) Substrate specificity.** The enzyme was able to hydrolyze pNPG but showed no activity toward pNP-α-substituted hexoses such as D-glucose, D-mannose, L-rhamnose, or *N*-acetyl-D-galactosaminide. pNP-β-substituted hexoses such as D-galactose, D-glucose, and D-mannose did not support catalysis, nor did the pentose pNP-β-D-xylopyranoside. Of the tested artificial substrates, only pNP-β-L-arabinopyranoside was hydrolyzed by the enzyme. However, the Michaelis-Menten constant for this substrate was very high ($K_m$, 37.4 ± 2.2 mM) compared to that of pNPG ($K_m$, 0.08 ± 0.01 mM). Of the natural substrates tested, the α-Gal was most active on the trisaccharide raffinose (2.9 U/mg), followed by the disaccharide melibiose (2.6 U/mg), and the tetrasaccharide stachyose (1.2 U/mg).

**(ii) Catalytic and stability properties.** Activity assays in a range of pH values indicated that the enzyme is more than 50% active between pH 4.1 and 6.7 and that it has a sharp optimum at pH 5.0 (Fig. 2, top). When the assay temperature was varied, optimal α-Gal activity was found at 90°C, while the enzyme was 50% active at a more physiological temperature of 75°C (Fig. 2, middle). GalS was completely inactive at temperatures below 50°C. At its optimal temperature for catalysis, the enzyme showed a half-life of 30 min (Fig. 2, bottom). At 70 or 80°C, the enzyme did not show any significant decrease in activity during 2.5 h of incubation.

**(iii) Inhibition of activity.** The α-Gal was tested for inactivation by divalent cations at a concentration of 10 mM. Most metal ions completely inhibited the activity of the enzyme ($Ag^{2+}$, $Ca^{2+}$, $Cd^{2+}$, $Co^{2+}$, $Cu^{2+}$, $Hg^{2+}$, $Mn^{2+}$, $Ni^{2+}$, and $Zn^{2+}$), but $Mg^{2+}$ and $Mo^{2+}$ had no effect. Assays in the presence of the divalent cation chelator EDTA or the reducing agent DTT did not alter the activity. Enzyme activity was also unaffected in the presence of several saccharides, such as D-galactose, L-arabinose, D-fucose, and sucrose, up to concentrations of 20 mM.

**Recombinant GalS overexpression.** The *galS* gene (Sso3127; Uniprot, Q97U94) was cloned in a T7 RNA polymerase-based vector and overexpressed *E. coli* BL21(DE3)-RIL. The heat-treated soluble fraction confirmed the presence of α-Gal activity at 80°C in the *galS* extract. Activity of *E. coli* transformants was also observed on selective plates containing 20 μg/ml of the chromogenic substrate X-α-Gal after a short incubation at 60°C. However, the soluble expression levels were too low to conduct any detailed experimental studies. Therefore, an orthologous gene from *S. tokodaii* (*galSt*, St2554, Q96XG2) was cloned and expressed, yielding an enzyme with characteristics and expression levels similar to the *S. solfataricus* α-Gal. Several reported strategies were then employed to obtain a sufficient amount of soluble recombinant protein. These included monitoring the protein overexpression levels over time (1, 2, 5, and 8 h and overnight induction); lowering the temperature during overnight protein overexpression (15, 20, and 25°C); decreasing the IPTG concentration (0.01, 0.05, and 0.1 mM); and changing the cell lysis buffer, the pH, and the ionic strength (HEPES-KOH, Tris-HCl, $NaP_i$, pH 5 to 10; ionic strength, 0 to 0.5 M NaCl), but none of these strategies

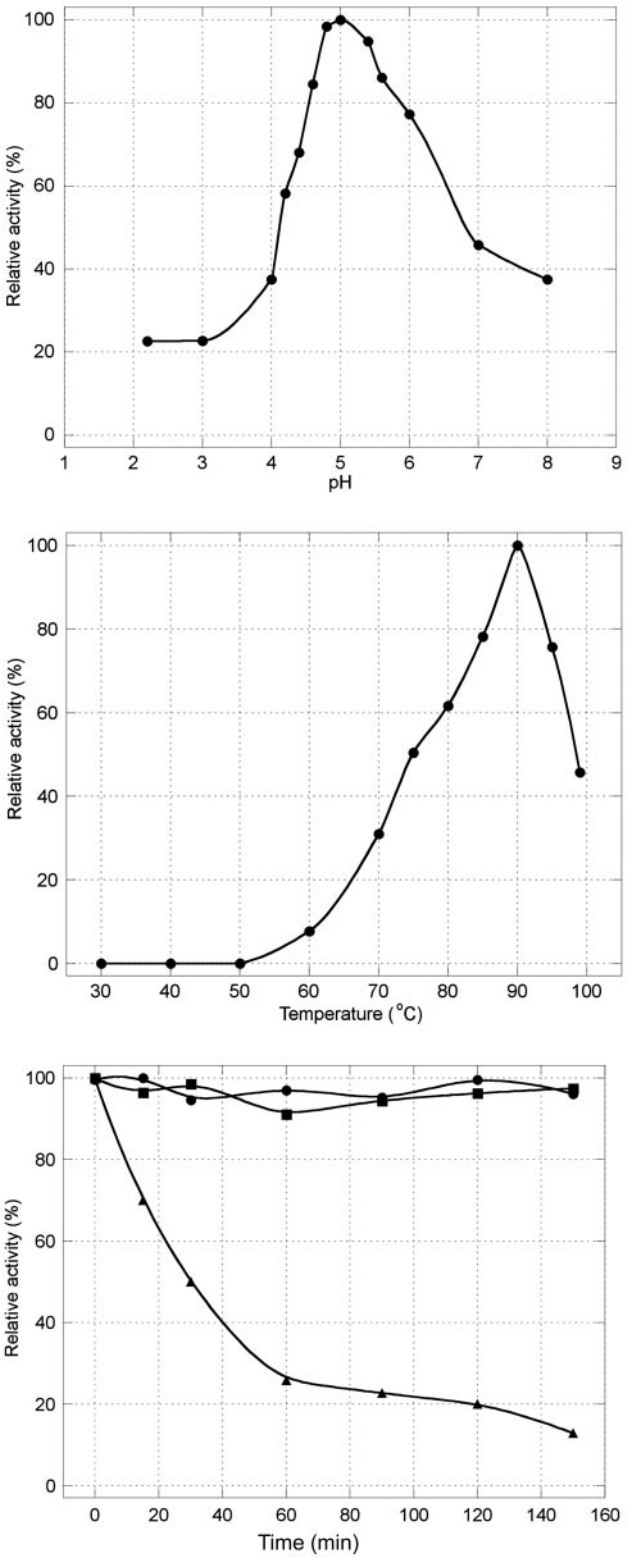


FIG. 2. Properties of the native GalS. Relative reaction rates as a function of pH (top) and temperature (middle). (Bottom) Thermal inactivation curves. Residual activity is given after preincubation at 70°C (●), 80°C (■), and 90°C (▲).

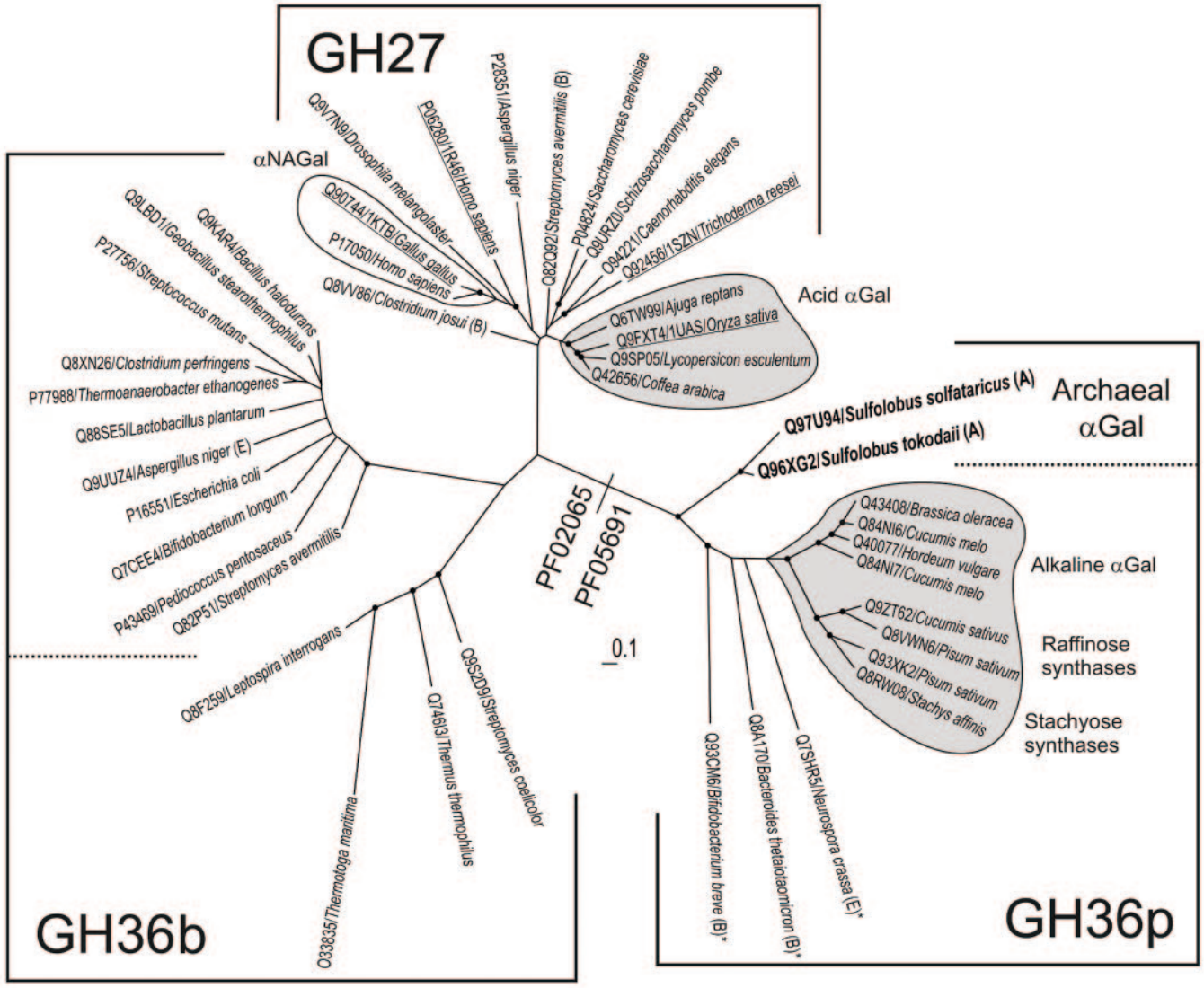


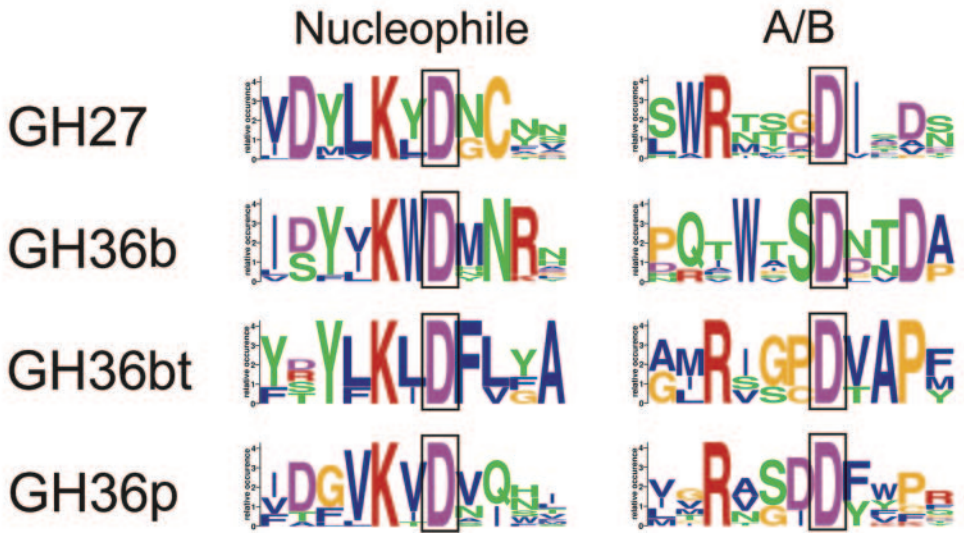


FIG. 3. (Top) Unrooted neighbor-joining tree of the catalytic domain of a representative set of α-Gals belonging to GH-D (for alignments, see Fig. S1 in the supplemental material). Nodes with bootstrap probabilities of >70% are indicated by dots. The scale bar indicates an evolutionary distance of 0.1 substitutions per position. Gray fields indicate sequences from a plant origin. Abbreviations: E, eukaryal sequences; B, bacterial

prevented the formation of inclusion bodies. However, since it is known that the *E. coli* MBP promotes the solubility of proteins to which it is fused (25), this strategy was also tested. The MBP was translationally fused to the N terminus of GalS, giving rise to a 116-kDa fusion protein. Overexpression in *E. coli* HB101 now yielded much more soluble fusion protein, which could easily be isolated by amylose affinity purification and subsequent anion exchange chromatography (Fig. 1, bottom).

The catalytic properties of the *E. coli*-produced GalS were comparable to those determined for the native enzyme. The Michaelis-Menten constants $K_m$ and $V_{max}$ for hydrolysis of pNPG were 0.085 ± 0.009 mM and 48.3 ± 1.1 U · $mg^{-1}$, respectively. The catalytic efficiency of the *E. coli*-produced GalS was 703.6 ± 15.7 $s^{-1} \cdot mM^{-1}$.

**Phylogeny of α-Gals and prediction of their catalytic amino acids.** GHs and transglycosidases are classified into families based on their sequence similarities (23). Family 27, which mainly contains α-Gals (EC 3.2.1.22) and α-*N*-acetylgalactosaminidases (EC 3.2.1.49), is related to family 36, which additionally consists of stachyose synthases (EC 2.4.1.67) and raffinose synthases (EC 2.4.1.82). Both families make up GH-D, and their catalytic domain adopts a common $(\beta\alpha)_8$-barrel fold (23). This prediction was recently confirmed by the elucidation of four structures of members of GH27 (16, 18–20). In order to analyze the diversity of both families and to position the *Sulfolobus* α-Gal sequences in a phylogenetic tree, we aligned the catalytic domains of 43 representative members of GH-D (for the alignment, see Fig. S1 in the supplemental material). A phylogenetic tree, which is shown in Fig. 3 (top), was constructed from this alignment. The tree indicates that α-Gals of clan GH-D can be divided into at least three major types: the eukaryal type (GH27), the bacterial type (GH36b), and a type consisting of mainly plant enzymes (GH36p). The latter type additionally comprises uncharacterized sequences from the *Archaea*, intestinal bacteria, and a fungus. The two *Sulfolobus* α-Gal sequences form the deepest branch of this plant subfamily and, as yet, constitute the only archaeal sequences of clan GH-D. Moreover, the *Sulfolobus* sequences are clearly distinct from other thermostable α-Gals that are produced by thermophilic bacteria, such as those from the genera *Thermotoga* (Uniprot, O33835) (33), *Thermus* (Q746I3) (15), and *Geobacillus* (Q9LBD1) (14).

The catalytic domain of GH-D members comprises only 241 of the 648 amino acids of the total GalS sequence (amino acids 225 to 466). It is encompassed by a 26-kDa N-terminal domain and a 21-kDa C-terminal domain of unknown functions. These extra domains are partly shared by members of GH36p (PF05691, raffinose synthase domain) but not by GH27 or GH36b members (PF02065, melibiase domain).

Figure 3B depicts the invariant aspartic acid residues that are predicted to be involved in catalysis as either the nucleophile or the acid/base (A/B) of the double displacement reaction mechanism of α-galactosyl hydrolysis. The prediction is based on the alignment combined with experimental and structural evidence for the nucleophile and A/B, which are available for GH27 (16, 18–20, 22, 35). While the sequence motif for the catalytic nucleophile is fully conserved within GH-D (K[Y/V/L/W]**D** [catalytic Asp in boldface]), the motif comprising the A/B aspartic acid is much less conserved (RXXX**D**) and has therefore been missed in previous analyses. The mesophilic bacterial α-Gal group seems to deviate most from the main A/B consensus but appears to contain another motif (**D**XXD) which is mutually shared with GH27. Yet another motif that is strongly conserved among α-Gals comprises two invariant aspartic acids that are involved in substrate binding of the C-4 and C-6 OH groups of D-galactose (16, 20). These residues have long been assumed to be involved in catalysis as the A/B residues. Interestingly, members of GH27 and GH36 can be distinguished on the bases of either a DDC or a DDG motif at this position, respectively. The cysteine of GH27 is fully conserved, since it is involved in the formation of a disulfide bond within the active site (see Fig. S1 in the supplemental material).

**Verification of the predicted catalytic amino acids.** The predicted nucleophilic and A/B aspartic acids of GalS were changed into glycines, yielding mutants D367G and D425G, respectively. The wild-type and both mutant enzymes were produced and purified. Activity assays using various substrate concentrations indicated that the activity of mutant D367G was below the detection limit ($<1 \times 10^{-3}$ times that of the wild type), whereas mutant D425G showed approximately $5 \times 10^{-3}$ times the activity of the wild type (data not shown). Molar concentrations of sodium azide or sodium formate were unable to restore or increase the activity of the mutant enzymes (data not shown).

## DISCUSSION

In the present study we have identified a novel thermostable α-Gal in cell extracts of the hyperthermophilic crenarchaeon *S. solfataricus* and studied the biochemical properties of the enzyme. Sequence analysis revealed an unusual phylogenetic position within the widely distributed class of GH-D α-Gals.

**Properties of GalS.** GalS and GalSt belong to the most thermoactive α-Gals known to date. Despite the fact that their primary sequence is very different from the α-Gals of thermophilic bacteria, their catalytic properties, such as the optimal pH of 5 and the optimal temperature of catalysis of 90°C, are similar. Interestingly, most related enzymes belonging to GH36p have neutral or slightly alkaline pH optima. This might be due to the fact that these enzymes contain an aspartic acid residue that is in juxtaposition to the predicted A/B residue, which may cause an increase in the $pK_a$ of the A/B. Catalysis can proceed only when the correct protonation state of the A/B is achieved, which may thus be at slightly higher pH.

sequences; A, archaeal sequences. Asterisks indicate uncharacterized sequences. (Bottom) Weblogo representations of the predicted catalytic amino acid sequence motifs of the different classes of GH-D. Character sizes indicate the relative occurrences of amino acids in the sequences encompassing the catalytic aspartic acids (boxed). The thermophilic bacterial sequences from the *Thermus* and *Thermotoga* subgroup are indicated by GH36bt; the other groups are defined as depicted in panel A. The full alignment of the catalytic domain, which indicates the mutated aspartic acids of GalS, is given in Fig. S1 in the supplemental material.

Since GalS contains an isoleucine residue at the corresponding position, its optimum activity may therefore be at a slightly acidic pH.

GalS is specific for α-linked D-galactosides and β-linked L-arabinosides. However, the Michaelis-Menten constant $K_m$, which is roughly the inverse measure of the enzyme's substrate affinity, is approximately 460 times lower for pNPG than for pNP-β-L-arabinoside, which probably excludes a physiological role of GalS as an arabinosidase. The activity on β-linked L-arabinoside is not surprising since it has identical configurations of the hydroxyl groups at C-1, C-2, C-3, and C-4 but lacks the $CH_2OH$ at its C-5 atom in comparison with galactose (11). Activity assays using the natural substrates melibiose, raffinose, and stachyose indicated that the enzyme can release D-galactose from oligosaccharides up to at least four sugar moieties, with the maximum catalytic rates on the trisaccharide. Several related alkaline α-Gals were reported to prefer the longer raffinose-type oligosaccharides (4, 17, 31). The enzyme showed no product inhibition, but it was severely inhibited by several divalent metal ions. This strong inhibitory effect of transition metal ions, such as $Zn^{2+}$, $Mn^{2+}$, and $Hg^{2+}$, was also observed with the raffinose synthase from *Vicia faba* seeds (32). Similarly, the raffinose synthase from *Pisum sativum* (Uniprot, Q8VWN6) was only 30.2% active after 1 h of incubation with 1 mM $NiCl_2$ (39). This finding suggests the presence of an oxidizable group, such as a free cysteine, that is required for substrate binding or catalysis.

**Mechanism of catalysis.** Based on sequence similarity with GH27, GH36 members are assumed to hydrolyze the glycosidic bond with retention of configuration of the released D-galactose (3). Although this assumption has never been experimentally verified, it is highly likely that GH36 enzymes retain instead of invert enzymes, since only the covalent enzyme galactose intermediate of the retaining mechanism will allow transglycosylation reactions to occur. The raffinose and stachyose synthases of GH36p make use of this principle by coupling the galactose moiety of galactinol to an incoming sucrose or raffinose molecule in the second stage of the reaction, respectively (39).

Mutagenesis of the proposed nucleophilic and A/B aspartic acids of GalS gave rise to similar protein yields, indicating properly folded proteins but virtually inactive enzymes. Although many mutations may have a near lethal effect on enzymatic activity, this finding, combined with sequence alignment data, suggests that both substituted aspartic acids are involved in α-galactosyl hydrolysis. Unfortunately, reactivation experiments with external nucleophiles such as azide and formate failed to restore the activity of either the nucleophile or the A/B mutant enzymes. While β-glycosidases can sometimes be reactivated up to wild-type levels (37), for unknown reasons this strategy seems to be far less efficient for retaining α-glycosidases (6, 9).

Catalytic residues of glycosidases can also be identified by an approach that consists of covalent modification of either the nucleophile or A/B, followed by mass spectrometric analysis of tryptic digests of the modified enzyme. This method requires specifically designed enzyme inhibitor molecules that create a stable bond between the enzyme and inhibitor. Using this strategy, the nucleophilic aspartic acid of the GH27 α-Gals from *Phanerochaete chrysosporium* and *Coffea arabica* (Uniprot, Q42656) was identified (22, 35).

**Metabolism of α-linked galactosides.** The ability to use α-linked galactosides such as melibiose and raffinose as a sole carbon and energy source implies that an organism should at least have a suitable sugar uptake system, an α-Gal, and an efficient catabolic pathway for the liberated monosaccharides. Within the *Sulfolobus* genus, the α-Gal described here was found only in the complete genome sequences of *S. solfataricus* (41) and *S. tokodaii* (27), not in *S. acidocaldarius* (5). This observation correlates well with the ability of *S. solfataricus* and *S. tokodaii*, but not *S. acidocaldarius*, to grow on melibiose and raffinose and also the monosaccharide D-galactose (21, 44). In addition, cellular growth on raffinose and D-galactose was also observed with *S. shibatae*, *S. yangmingensis*, and *S. tengchongensis*, which may imply that these species have an α-Gal gene in their genomes as well (21, 24, 45).

To date, two primary catabolic pathways for D-galactose have been reported. Most ubiquitous is the Leloir pathway, in which galactose is converted to glucose-1-phosphate by the action of a sugar kinase, uridylyltransferase, and an epimerase (13). Galactose can also be degraded according to a scheme that was originally proposed by De Ley and Doudoroff (10). In this pathway, D-galactose is oxidized to D-galactonate, subsequently dehydrated to 2-keto-3-deoxy-D-galactonate, phosphorylated at the C-6 position, and cleaved by an aldolase to yield pyruvate and D-glyceraldehyde-3-phosphate. *S. solfataricus* was recently demonstrated to use this pathway by employing a promiscuous enzyme set that can convert both D-galactose and D-glucose, as well as their derivatives (29, 30). Since the aldolase can convert nonphosphorylated substrates, the pathway may also occur nonphosphorylatively in vivo.

## ACKNOWLEDGMENTS

This work was supported by a grant from the European Union in the framework of the SCREEN project (contract QLK3-CT-2000-00649). A.P.L.S. thanks the University of Sheffield and the United Kingdom's Engineering and Physical Sciences Research Council (EPSRC) for a scholarship. P.C.W. thanks the EPSRC for provision of an Advanced Research Fellowship (GR/A11311/01).

## REFERENCES

1. **Boyer, H. W., and R. Rouland-Dussoix.** 1969. A complementation analysis of the restriction and modification of DNA in *Escherichia coli*. J. Mol. Biol. **41:**459–472.
2. **Brock, T. D., K. M. Brock, R. T. Belly, and R. L. Weiss.** 1972. *Sulfolobus*: a new genus of sulfur-oxidizing bacteria living at low pH and high temperature. Arch. Mikrobiol. **84:**54–68.
3. **Brumer, H., III, P. F. Sims, and M. L. Sinnott.** 1999. Lignocellulose degradation by *Phanerochaete chrysosporium*: purification and characterization of the main alpha-galactosidase. Biochem. J. **339:**43–53.
4. **Carmi, N., G. Zhang, M. Petreikov, Z. Gao, Y. Eyal, D. Granot, and A. A. Schaffer.** 2003. Cloning and functional expression of alkaline alpha-galactosidase from melon fruit: similarity to plant SIP proteins uncovers a novel family of plant glycosyl hydrolases. Plant J. **33:**97–106.
5. **Chen, L., K. Brugger, M. Skovgaard, P. Redder, Q. She, E. Torarinsson, B. Greve, M. Awayez, A. Zibat, H. P. Klenk, and R. A. Garrett.** 2005. The genome of *Sulfolobus acidocaldarius*, a model organism of the *Crenarchaeota*. J. Bacteriol. **187:**4992–4999.
6. **Cobucci-Ponzano, B., A. Trincone, A. Giordano, M. Rossi, and M. Moracci.** 2003. Identification of the catalytic nucleophile of the family 29 alpha-L-fucosidase from *Sulfolobus solfataricus* via chemical rescue of an inactive mutant. Biochemistry **42:**9525–9531.
7. **Constantinesco, F., P. Forterre, and C. Elie.** 2002. NurA, a novel 5′-3′ nuclease gene linked to rad50 and mre11 homologs of thermophilic Archaea. EMBO Rep. **3:**537–542.
8. **Crooks, G. E., G. Hon, J. M. Chandonia, and S. E. Brenner.** 2004. WebLogo: a sequence logo generator. Genome Res. **14:**1188–1190.

9. **Debeche, T., C. Bliard, P. Debeire, and M. J. O'Donohue.** 2002. Probing the catalytically essential residues of the alpha-L-arabinofuranosidase from *Thermobacillus xylanilyticus*. Protein Eng. **15:**21–28.
10. **De Ley, J., and M. Doudoroff.** 1957. The metabolism of D-galactose in *Pseudomonas saccharophila*. J. Biol. Chem. **227:**745–757.
11. **Dey, P. M., and J. B. Pridham.** 1972. Biochemistry of alpha-galactosidases. Adv. Enzymol. Relat. Areas Mol. Biol. **36:**91–130.
12. **Fabry, J.** 1898. Ein Beitrag Zur Kenntnis der Purpura haemorrhagica nodularis (Purpura papulosa hemorrhagica Hebrae). Arch. Dermatol. Syphilol. **43:**187–200.
13. **Frey, P. A.** 1996. The Leloir pathway: a mechanistic imperative for three enzymes to change the stereochemical configuration of a single carbon in galactose. FASEB J. **10:**461–470.
14. **Fridjonsson, O., H. Watzlawick, A. Gehweiler, and R. Mattes.** 1999. Thermostable alpha-galactosidase from *Bacillus stearothermophilus* NUB3621: cloning, sequencing and characterization. FEMS Microbiol. Lett. **176:**147–153.
15. **Fridjonsson, O., H. Watzlawick, A. Gehweiler, T. Rohrhirsch, and R. Mattes.** 1999. Cloning of the gene encoding a novel thermostable alpha-galactosidase from *Thermus brockianus* ITI360. Appl. Environ. Microbiol. **65:**3955–3963.
16. **Fujimoto, Z., S. Kaneko, M. Momma, H. Kobayashi, and H. Mizuno.** 2003. Crystal structure of rice alpha-galactosidase complexed with D-galactose. J. Biol. Chem. **278:**20313–20318.
17. **Gao, Z., and A. A. Schaffer.** 1999. A novel alkaline alpha-galactosidase from melon fruit with a substrate preference for raffinose. Plant Physiol. **119:**979–988.
18. **Garman, S. C., and D. N. Garboczi.** 2004. The molecular defect leading to Fabry disease: structure of human alpha-galactosidase. J. Mol. Biol. **337:**319–335.
19. **Garman, S. C., L. Hannick, A. Zhu, and D. N. Garboczi.** 2002. The 1.9 A structure of alpha-*N*-acetylgalactosaminidase: molecular basis of glycosidase deficiency diseases. Structure **10:**425–434.
20. **Golubev, A. M., R. A. Nagem, J. R. Brandao Neto, K. N. Neustroev, E. V. Eneyskaya, A. A. Kulminskaya, K. A. Shabalin, A. N. Savel'ev, and I. Polikarpov.** 2004. Crystal structure of alpha-galactosidase from *Trichoderma reesei* and its complex with galactose: implications for catalytic mechanism. J. Mol. Biol. **339:**413–422.
21. **Grogan, D. W.** 1989. Phenotypic characterization of the archaebacterial genus *Sulfolobus*: comparison of five wild-type strains. J. Bacteriol. **171:**6710–6719.
22. **Hart, D. O., S. He, C. J. Chany II, S. G. Withers, P. F. Sims, M. L. Sinnott, and H. Brumer III.** 2000. Identification of Asp-130 as the catalytic nucleophile in the main alpha-galactosidase from *Phanerochaete chrysosporium*, a family 27 glycosyl hydrolase. Biochemistry **39:**9826–9836.
23. **Henrissat, B.** 1991. A classification of glycosyl hydrolases based on amino acid sequence similarities. Biochem. J. **280:**309–316.
24. **Jan, R. L., J. Wu, S. M. Chaw, C. W. Tsai, and S. D. Tsen.** 1999. A novel species of thermoacidophilic archaeon, *Sulfolobus yangmingensis* sp. nov. Int. J. Syst. Bacteriol. **49:**1809–1816.
25. **Kapust, R. B., and D. S. Waugh.** 1999. *Escherichia coli* maltose-binding protein is uncommonly effective at promoting the solubility of polypeptides to which it is fused. Protein Sci. **8:**1668–1674.
26. **Kardinahl, S., C. L. Schmidt, T. Hansen, S. Anemuller, A. Petersen, and G. Schafer.** 1999. The strict molybdate-dependence of glucose-degradation by the thermoacidophile *Sulfolobus acidocaldarius* reveals the first crenarchaeotic molybdenum containing enzyme—an aldehyde oxidoreductase. Eur. J. Biochem. **260:**540–548.
27. **Kawarabayasi, Y., Y. Hino, H. Horikawa, K. Jin-No, M. Takahashi, M. Sekine, S. Baba, A. Ankai, H. Kosugi, A. Hosoyama, S. Fukui, Y. Nagai, K. Nishijima, R. Otsuka, H. Nakazawa, M. Takamiya, Y. Kato, T. Yoshizawa, T. Tanaka, Y. Kudoh, J. Yamazaki, N. Kushida, A. Oguchi, K. Aoki, S. Masuda, M. Yanagii, M. Nishimura, A. Yamagishi, T. Oshima, and H. Kikuchi.** 2001. Complete genome sequence of an aerobic thermoacidophilic crenarchaeon, Sulfolobus tokodaii strain7. DNA Res. **8:**123–140.
28. **Keller, F., and M. Pharr.** 1996. Metabolism of carbohydrates in sinks and sources: galactosyl-sucrose oligosaccharides, p. 157–183. *In* E. Zamski and A. A. Schafer (ed.), Photoassimilate distribution in plants and crops. Marcel Dekker, New York, N.Y.
29. **Lamble, H. J., N. I. Heyer, S. D. Bull, D. W. Hough, and M. J. Danson.** 2003. Metabolic pathway promiscuity in the archaeon *Sulfolobus solfataricus* revealed by studies on glucose dehydrogenase and 2-keto-3-deoxygluconate aldolase. J. Biol. Chem. **278:**34066–34072.
30. **Lamble, H. J., A. Theodossis, C. C. Milburn, G. L. Taylor, S. D. Bull, D. W. Hough, and M. J. Danson.** 2005. Promiscuity in the part-phosphorylative Entner-Doudoroff pathway of the archaeon *Sulfolobus solfataricus*. FEBS Lett. **579:**6865–6869.
31. **Lee, R. H., M. C. Lin, and S. C. Chen.** 2004. A novel alkaline alpha-galactosidase gene is involved in rice leaf senescence. Plant Mol. Biol. **55:**281–295.
32. **Lehle, L., and W. Tanner.** 1973. The function of myo-inositol in the biosynthesis of raffinose. Purification and characterization of galactinol:sucrose 6-galactosyltransferase from *Vicia faba* seeds. Eur. J. Biochem. **38:**103–110.
33. **Liebl, W., B. Wagner, and J. Schellhase.** 1998. Properties of an alpha-galactosidase, and structure of its gene galA, within an alpha- and beta-galactoside utilization gene cluster of the hyperthermophilic bacterium *Thermotoga maritima*. Syst. Appl. Microbiol. **21:**1–11.
34. **Lieshout, J. F. T., C. H. Verhees, T. J. G. Ettema, S. Van der Sar, H. Imamura, H. Matsuzawa, J. Van der Oost, and W. M. De Vos.** 2003. Identification and molecular characterization of a novel type of alpha-galactosidase from *Pyrococcus furiosus*. Biocatal. Biotransformation **21:**243–252.
35. **Ly, H. D., S. Howard, K. Shum, S. He, A. Zhu, and S. G. Withers.** 2000. The synthesis, testing and use of 5-fluoro-alpha-D-galactosyl fluoride to trap an intermediate on green coffee bean alpha-galactosidase and identify the catalytic nucleophile. Carbohydr. Res. **329:**539–547.
36. **McIlvaine, T. C.** 1921. A buffer solution for colorimetric comparison. J. Biol. Chem. **49:**183–186.
37. **Moracci, M., A. Trincone, G. Perugino, M. Ciaramella, and M. Rossi.** 1998. Restoration of the activity of active-site mutants of the hyperthermophilic beta-glycosidase from *Sulfolobus solfataricus*: dependence of the mechanism on the action of external nucleophiles. Biochemistry **37:**17262–17270.
38. **Notredame, C., D. G. Higgins, and J. Heringa.** 2000. T-Coffee: a novel method for fast and accurate multiple sequence alignment. J. Mol. Biol. **302:**205–217.
39. **Peterbauer, T., L. Mach, J. Mucha, and A. Richter.** 2002. Functional expression of a cDNA encoding pea (*Pisum sativum* L.) raffinose synthase, partial purification of the enzyme from maturing seeds, and steady-state kinetic analysis of raffinose synthesis. Planta **215:**839–846.
40. **Pitcher, D. G., N. A. Saunders, and R. J. Owen.** 1989. Rapid extraction of bacterial genomic DNA with guanidium thiocyanate. Lett. Appl. Microbiol. **8:**151–156.
41. **She, Q., R. K. Singh, F. Confalonieri, Y. Zivanovic, G. Allard, M. J. Awayez, C. C. Chan-Weiher, I. G. Clausen, B. A. Curtis, A. De Moors, G. Erauso, C. Fletcher, P. M. Gordon, I. Heikamp-de Jong, A. C. Jeffries, C. J. Kozera, N. Medina, X. Peng, H. P. Thi-Ngoc, P. Redder, M. E. Schenk, C. Theriault, N. Tolstrup, R. L. Charlebois, W. F. Doolittle, M. Duguet, T. Gaasterland, R. A. Garrett, M. A. Ragan, C. W. Sensen, and J. Van der Oost.** 2001. The complete genome of the crenarchaeon *Sulfolobus solfataricus* P2. Proc. Natl. Acad. Sci. USA **98:**7835–7840.
42. **Snijders, A. P., M. G. de Vos, B. de Koning, and P. C. Wright.** 2005. A fast method for quantitative proteomics based on a combination between two-dimensional electrophoresis and (15)N-metabolic labelling. Electrophoresis **26:**3191–3199.
43. **Snijders, A. P., M. G. de Vos, and P. C. Wright.** 2005. Novel approach for peptide quantitation and sequencing based on 15N and 13C metabolic labeling. J. Proteome Res. **4:**578–585.
44. **Suzuki, T., T. Iwasaki, T. Uzawa, K. Hara, N. Nemoto, T. Kon, T. Ueki, A. Yamagishi, and T. Oshima.** 2002. *Sulfolobus tokodaii* sp. nov. (*f. Sulfolobus* sp. strain 7), a new member of the genus *Sulfolobus* isolated from Beppu Hot Springs, Japan. Extremophiles **6:**39–44.
45. **Xiang, X., X. Dong, and L. Huang.** 2003. *Sulfolobus tengchongensis* sp. nov., a novel thermoacidophilic archaeon isolated from a hot spring in Tengchong, China. Extremophiles **7:**493–498.
46. **Zillig, W., K. O. Stetter, S. Wunderl, W. Schulz, H. Priess, and I. Scholz.** 1980. The *Sulfolobus*-"*Caldariella*" group: taxonomy on the basis of the structure of DNA-dependent RNA polymerases. Arch. Mikrobiol. **125:**259–269.